# Discontinuous Galerkin methods for the Boltzmann-Poisson systems in semiconductor device simulations

Yingda Cheng, Irene M. Gamba, Armando Majorana, and Chi-Wang Shu

Citation: AIP Conference Proceedings **1333**, 890 (2011); doi: 10.1063/1.3562758
View online: http://dx.doi.org/10.1063/1.3562758
View Table of Contents: http://scitation.aip.org/content/aip/proceeding/aipcp/1333?ver=pdfcov
Published by the AIP Publishing

# Discontinuous Galerkin methods for the Boltzmann-Poisson systems in semiconductor device simulations

Yingda Cheng[*], Irene M. Gamba[†], Armando Majorana[**] and Chi-Wang Shu[‡]

[*]*Department of Mathematics and ICES, University of Texas, Austin, TX 78712, USA. ycheng@math.utexas.edu.*
[†]*Department of Mathematics and ICES, University of Texas, Austin, TX 78712, USA. gamba@math.utexas.edu.*
[**]*Dipartimento di Matematica e Informatica, Università di Catania, Catania, Italy. majorana@dmi.unict.it.*
[‡]*Division of Applied Mathematics, Brown University, Providence, RI 02912, USA. shu@dam.brown.edu.*

**Abstract.** We are interested in the deterministic computation of the transients for the Boltzmann-Poisson system describing electron transport in semiconductor devices. The main difficulty of such computation arises from the very high dimensions of the model, making it necessary to use relatively coarse meshes and hence requiring the numerical solver to be stable and to have good resolution under coarse meshes. In this paper we consider the discontinuous Galerkin (DG) method, which is a finite element method using discontinuous piecewise polynomials as basis functions and numerical fluxes based on upwinding for stability, for solving the Boltzmann-Poisson system. In many situations, the deterministic DG solver can produce accurate solutions with equal or less CPU time than the traditional DSMC (Direct Simulation Monte Carlo) solvers. Numerical simulation results on a diode and a 2D double-gate MOSFET are given.

**Keywords:** Semiconductor device simulation, Boltzmann-Poisson, discontinuous Galerkin
**PACS:** 85, 89

## INTRODUCTION

In modern semiconductor device simulations, the classical macroscopic models, such as drift diffusion, energy transport models, are not adequate to capture the subtle kinetic effects that happen in nano-scales. The semiclassical Boltzmann transport equation (BTE) coupled with the Poisson equation serves as a general theoretical framework for modeling carrier transports for sub-micron devices. The BTE has a hyperbolic component of transport and a dissipative mechanism due to the collision operator. Its solutions are positive probability distributions. To solve this system by deterministic numerical schemes is very costly, because the full Boltzmann equation is an integro-differential equation of very high dimensions (3D is space and 3D in phase plus time for real devices). This heavy computational cost explains why the BP system is traditionally simulated by the Direct Simulation Monte Carlo (DSMC) methods. DSMC methods have the advantage that the increase in computational cost is not significant with the increase of dimensions. However, the simulation results are often noisy, and it is difficult to compute transient details (time dependent states), especially if the probability density function (*pdf*) is desired. In recent years, deterministic solvers to the BP system were considered in the literature, see for example [1, 2, 3, 4]. These methods provide accurate results which, in general, agree well with those obtained from DSMC simulations, sometimes at a comparable or even less computational time. Deterministic solvers have the distinct advantage in resolving transient details for the *pdf*. However, the main difficulty of the deterministic solvers arises from the very high dimensions of the model, making it necessary to use relatively coarse meshes and hence requiring the numerical solver to be stable and to have good resolution under coarse meshes. This can be challenging because under coarse meshes, for a convection dominated problem, the solution may contain high gradient (relative to the mesh) regions, which may lead to instability if care is not taken in the design of the algorithm. One class of very successful numerical solvers for the deterministic solvers of the BP system is the weighted essentially non-oscillatory (WENO) finite difference scheme [3, 4]. The advantage of the WENO scheme is that it is relatively simple to code and very stable even on coarse meshes for solutions containing sharp gradient regions. However, the WENO finite difference method requires smooth meshes to achieve high order accuracy, hence it is not very flexible for adaptive meshes.

On the other hand, the Runge-Kutta discontinuous Galerkin (RKDG) method, which is a class of finite element methods originally devised to solve hyperbolic conservation laws (see [5] for a review), is a suitable alternative for solving the BP system. Using a completely discontinuous polynomial space for both the test and trial functions in the spatial variables and coupled with explicit and nonlinearly stable high order Runge-Kutta time discretization, the

*27th International Symposium on Rarefied Gas Dynamics, 2010*
AIP Conf. Proc. 1333, 890-895 (2011); doi: 10.1063/1.3562758

method has the advantage of flexibility for arbitrarily unstructured meshes, with a compact stencil, and with the ability to easily accommodate arbitrary *hp*-adaptivity. In recent years, we have initialized a line of research to develop and implement the RKDG method, coupled with the local DG (LDG) solution for the Poisson equation, for solving the full BP system, see [7, 8, 9, 10]. It is demonstrated through extensive numerical studies that the DG solver produces good resolution on relatively coarse meshes for the transient and steady state *pdf*, as well as various orders of moments and the current-voltage characteristics (*I-V* curves), which compare well with DSMC results. Our DG solver has the capability of handling full energy bands [9] that no other deterministic solver has been able to implement so far.

## THE BOLTZMANN-POISSON SYSTEM

The evolution of the electron distribution function $f(\mathrm{t},\mathbf{x},\mathbf{k})$ in semiconductors, depending on the time t, position $\mathbf{x}$ and electron wave vector $\mathbf{k}$, is governed by the following BTE,

$$\frac{\partial f}{\partial \mathrm{t}} + \frac{1}{\hbar}\nabla_{\mathbf{k}}\,\varepsilon\cdot\nabla_{\mathbf{x}} f - \frac{q}{\hbar}\mathbf{E}\cdot\nabla_{\mathbf{k}} f = Q(f)\,, \tag{1}$$

where $\hbar$ is the reduced Planck constant, and $q$ denotes the positive elementary charge. The function $\varepsilon(\mathbf{k})$ is the energy of the considered crystal conduction band measured from the band minimum; according to the Kane dispersion relation, $\varepsilon$ is the positive root of

$$\varepsilon(1+\alpha\varepsilon) = \frac{\hbar^2 k^2}{2m^*}\,, \tag{2}$$

where $\alpha$ is the non-parabolicity factor and $m^*$ the effective electron mass. The electric field $\mathbf{E}$ is related to the doping density $N_D$ and the electron density $n$, which equals the zero-order moment of the electron distribution function $f$, by the Poisson equation

$$\nabla_{\mathbf{x}}\left[\varepsilon_r(\mathbf{x})\,\nabla_{\mathbf{x}} V\right] = \frac{q}{\varepsilon_0}\left[n(\mathrm{t},\mathbf{x}) - N_D(\mathbf{x})\right], \quad \mathbf{E} = -\nabla_{\mathbf{x}} V\,, \tag{3}$$

where $\varepsilon_0$ is the dielectric constant of the vacuum, $\varepsilon_r(\mathbf{x})$ labels the relative dielectric function depending on the semiconductor and $V$ is the electrostatic potential. For low electron densities, the collision operator $Q(f)$ is

$$Q(f)(\mathrm{t},\mathbf{x},\mathbf{k}) = \int_{\mathbb{R}^3}\left[S(\mathbf{k}',\mathbf{k})f(\mathrm{t},\mathbf{x},\mathbf{k}') - S(\mathbf{k},\mathbf{k}')f(\mathrm{t},\mathbf{x},\mathbf{k})\right]d\mathbf{k}', \tag{4}$$

where $S(\mathbf{k}',\mathbf{k})$ is the kernel depending on the scattering mechanisms between electrons and phonons in the semiconductor.

For the numerical treatment of the BP system, it is convenient to introduce suitable dimensionless quantities and variables. We assume $T_L = 300\,K$. Typical values for length, time and voltage are $\ell_* = 10^{-6}\,m$, $t_* = 10^{-12}\,s$ and $V_* = 1\,\mathrm{Volt}$, respectively. If we consider a two-dimensional device and three-dimensional $\mathbf{k}$ space, the dimensionless variables are

$$(x,y) = \frac{\mathbf{x}}{\ell_*}\,, \quad t = \frac{\mathrm{t}}{t_*}\,, \quad \Psi = \frac{V}{V_*}\,, \quad (E_x,E_y,0) = \frac{\mathbf{E}}{E_*}$$

with $E_* = 0.1\,V_*\,\ell_*^{-1}$ and

$$E_x = -c_v\frac{\partial\Psi}{\partial x}\,, \quad E_y = -c_v\frac{\partial\Psi}{\partial y}\,, \quad c_v = \frac{V_*}{\ell_* E_*}\,.$$

In correspondence to [2, 3], we perform a coordinate transformation for $\mathbf{k}$ according to

$$\mathbf{k} = \frac{\sqrt{2m^* k_B T_L}}{\hbar}\sqrt{w(1+\alpha_K w)}\left(\mu, \sqrt{1-\mu^2}\cos\varphi, \sqrt{1-\mu^2}\sin\varphi\right), \tag{5}$$

where the new independent variables are the dimensionless energy $w = \dfrac{\varepsilon}{k_B T_L}$, the cosine of the polar angle $\mu$ and the azimuth angle $\varphi$ with $\alpha_K = k_B T_L \alpha$. The distribution function under the transformation becomes

$$\Phi(t,x,y,w,\mu,\varphi) = s(w) f(\mathrm{t},\mathbf{x},\mathbf{k})\,,$$

where

$$s(w) = \sqrt{w(1+\alpha_K w)}(1+2\alpha_K w), \tag{6}$$

is proportional to the Jacobian of the change of variables (5) and, apart from a dimensional constant factor, to the density of states. The BTE becomes now,

$$\frac{\partial \Phi}{\partial t} + \frac{\partial}{\partial x}(g_1\Phi) + \frac{\partial}{\partial y}(g_2\Phi) + \frac{\partial}{\partial w}(g_3\Phi) + \frac{\partial}{\partial \mu}(g_4\Phi) + \frac{\partial}{\partial \varphi}(g_5\Phi) = C(\Phi)\,. \tag{7}$$

The functions $g_i$ $(i = 1,2,..,5)$ in the advection terms depend on the independent variables $w$, $\mu$, $\varphi$ as well as on time and position via the electric field. They are given by

$$\begin{aligned}
g_1(\cdot) &= c_x \frac{\mu\sqrt{w(1+\alpha_K w)}}{1+2\alpha_K w}\,,\\
g_2(\cdot) &= c_x \frac{\sqrt{1-\mu^2}\sqrt{w(1+\alpha_K w)}\cos\varphi}{1+2\alpha_K w}\,,\\
g_3(\cdot) &= -2c_k \frac{\sqrt{w(1+\alpha_K w)}}{1+2\alpha_K w}\left[\mu\, E_x(t,x,y) + \sqrt{1-\mu^2}\cos\varphi\, E_y(t,x,y)\right],\\
g_4(\cdot) &= -c_k \frac{\sqrt{1-\mu^2}}{\sqrt{w(1+\alpha_K w)}}\left[\sqrt{1-\mu^2}\, E_x(t,x,y) - \mu\cos\varphi\, E_y(t,x,y)\right],\\
g_5(\cdot) &= c_k \frac{\sin\varphi}{\sqrt{w(1+\alpha_K w)}\sqrt{1-\mu^2}}\, E_y(t,x,y)
\end{aligned}$$

with

$$c_x = \frac{t_*}{\ell_*}\sqrt{\frac{2k_BT_L}{m^*}} \text{ and } \quad c_k = \frac{t_* q E_*}{\sqrt{2m^* k_B T_L}}\,.$$

The right hand side of (7) is the integral-difference operator

$$C(\Phi)(t,x,y,w,\mu,\varphi) = s(w)\left\{\int_0^\pi d\varphi' \int_{-1}^1 d\mu' \left[c_+\Phi(t,x,y,w+\gamma,\mu',\varphi') + c_-\Phi(t,x,y,w-\gamma,\mu',\varphi')\right]\right.$$

$$\left. + c_0 \int_0^\pi d\varphi' \int_{-1}^1 d\mu'\, \Phi(t,x,y,w,\mu',\varphi')\right\} - 2\pi[c_0 s(w) + c_+ s(w-\gamma) + c_- s(w+\gamma)]\Phi(t,x,y,w,\mu,\varphi)\,,$$

where

$$(c_0, c_+, c_-) = \frac{2m^* t_*}{\hbar^3}\sqrt{2m^* k_B T_L}\,(K_0, (n_q+1)K, n_q K)\,, \quad \gamma = \frac{\hbar\omega_p}{k_B T_L}$$

are dimensionless parameters. The phonon frequency $\omega_p$ and the physical parameters $K$ and $K_0$ depend on the semiconductor material. The electron density becomes

$$n(t_*t, \ell_* x, \ell_* y) = \int_{\mathbb{R}^3} f(t_*t, \ell_* x, \ell_* y, \mathbf{k})\, d\mathbf{k} = \left(\frac{\sqrt{2m^* k_B T_L}}{\hbar}\right)^3 \rho(t,x,y)\,,$$

where

$$\rho(t,x,y) = \int_0^{+\infty} dw \int_{-1}^1 d\mu \int_0^\pi d\varphi\, \Phi(t,x,y,w,\mu,\varphi)\,. \tag{8}$$

Hence, the dimensionless Poisson equation is

$$\frac{\partial}{\partial x}\left(\varepsilon_r \frac{\partial \Psi}{\partial x}\right) + \frac{\partial}{\partial y}\left(\varepsilon_r \frac{\partial \Psi}{\partial y}\right) = c_p\left[\rho(t,x,y) - \mathcal{N}_D(x,y)\right] \tag{9}$$

with

$$\mathcal{N}_D(x,y) = \left(\frac{\sqrt{2m^* k_B T_L}}{\hbar}\right)^{-3} N_D(\ell_* x, \ell_* y) \text{ and } c_p = \left(\frac{\sqrt{2m^* k_B T_L}}{\hbar}\right)^3 \frac{\ell_*^2 q}{\varepsilon_0}\,.$$

## THE DG SOLVER

For simplicity of discussion, we implement our algorithm on a cartesian grid, although the DG methods work well on unstructured meshes as well. Suppose the grid is $\Omega_{ijkmn} = \left[x_{i-\frac{1}{2}}, x_{i+\frac{1}{2}}\right] \times \left[y_{j-\frac{1}{2}}, y_{j+\frac{1}{2}}\right] \times \left[w_{k-\frac{1}{2}}, w_{k+\frac{1}{2}}\right] \times \left[\mu_{m-\frac{1}{2}}, \mu_{m+\frac{1}{2}}\right] \times \left[\varphi_{n-\frac{1}{2}}, \varphi_{n+\frac{1}{2}}\right]$ where $i = 1,\ldots N_x,\ j = 1,\ldots N_y,\ k = 1,\ldots N_w,\ m = 1,\ldots N_\mu,\ n = 1,\ldots N_\varphi$, and $x_{i\pm\frac{1}{2}} = x_i \pm \frac{\Delta x_i}{2}, \quad y_{j\pm\frac{1}{2}} = y_j \pm \frac{\Delta y_j}{2}, \quad w_{k\pm\frac{1}{2}} = w_k \pm \frac{\Delta w_k}{2} \quad \mu_{m\pm\frac{1}{2}} = \mu_m \pm \frac{\Delta\mu_m}{2}, \quad \varphi_{n\pm\frac{1}{2}} = \varphi_n \pm \frac{\Delta\varphi_n}{2}$. The approximation functional space is defined as

$$V_h^\ell = \{v : v|_{\Omega_{ijkmn}} \in P^\ell(\Omega_{ijkmn})\}. \tag{10}$$

Here, $P^\ell(\Omega_{ijkmn})$ is the set of all polynomials of degree at most $\ell$ on $\Omega_{ijkmn}$. The DG formulation for the Boltzmann equation (7) would be: to find $\Phi_h \in V_h^\ell$, such that

$$\int_{\Omega_{ijkmn}} (\Phi_h)_t\, v_h\, d\Omega - \int_{\Omega_{ijkmn}} g_1 \Phi_h\,(v_h)_x\, d\Omega - \int_{\Omega_{ijkmn}} g_2 \Phi_h\,(v_h)_y\, d\Omega - \int_{\Omega_{ijkmn}} g_3 \Phi_h\,(v_h)_w\, d\Omega - \int_{\Omega_{ijkmn}} g_4 \Phi_h\,(v_h)_\mu\, d\Omega$$
$$- \int_{\Omega_{ijkmn}} g_5 \Phi_h\,(v_h)_\varphi\, d\Omega + F_x^+ - F_x^- + F_y^+ - F_y^- + F_w^+ - F_w^- + F_\mu^+ - F_\mu^- + F_\varphi^+ - F_\varphi^- = \int_{\Omega_{ijkmn}} C(\Phi_h)\, v_h\, d\Omega. \tag{11}$$

for any test function $v_h \in V_h^\ell$. In (11),

$F_x^\pm = \int_{y_{j-\frac{1}{2}}}^{y_{j+\frac{1}{2}}} \int_{w_{k-\frac{1}{2}}}^{w_{k+\frac{1}{2}}} \int_{\mu_{m-\frac{1}{2}}}^{\mu_{m+\frac{1}{2}}} \int_{\varphi_{n-\frac{1}{2}}}^{\varphi_{n+\frac{1}{2}}} g_1 \check{\Phi} v_h^\mp(x_{i\pm\frac{1}{2}}, y, w, \mu, \varphi) dy\, dw\, d\mu\, d\varphi,$

$F_y^\pm = \int_{x_{i-\frac{1}{2}}}^{x_{i+\frac{1}{2}}} \int_{w_{k-\frac{1}{2}}}^{w_{k+\frac{1}{2}}} \int_{\mu_{m-\frac{1}{2}}}^{\mu_{m+\frac{1}{2}}} \int_{\varphi_{n-\frac{1}{2}}}^{\varphi_{n+\frac{1}{2}}} g_2 \bar{\Phi} v_h^\mp(x, y_{j\pm\frac{1}{2}}, w, \mu, \varphi) dx\, dw\, d\mu\, d\varphi,$

$F_w^\pm = \int_{x_{i-\frac{1}{2}}}^{x_{i+\frac{1}{2}}} \int_{y_{j-\frac{1}{2}}}^{y_{j+\frac{1}{2}}} \int_{\mu_{m-\frac{1}{2}}}^{\mu_{m+\frac{1}{2}}} \int_{\varphi_{n-\frac{1}{2}}}^{\varphi_{n+\frac{1}{2}}} \widehat{g_3 \Phi} v_h^\mp(x, y, w_{k\pm\frac{1}{2}}, \mu, \varphi) dx\, dy\, d\mu\, d\varphi,$

$F_\mu^\pm = \int_{x_{i-\frac{1}{2}}}^{x_{i+\frac{1}{2}}} \int_{y_{j-\frac{1}{2}}}^{y_{j+\frac{1}{2}}} \int_{w_{k-\frac{1}{2}}}^{w_{k+\frac{1}{2}}} \int_{\varphi_{n-\frac{1}{2}}}^{\varphi_{n+\frac{1}{2}}} \widetilde{g_4 \Phi} v_h^\mp(x, y, w, \mu_{m\pm\frac{1}{2}}, \varphi) dx\, dy\, dw\, d\varphi,$

$F_\varphi^\pm = \int_{x_{i-\frac{1}{2}}}^{x_{i+\frac{1}{2}}} \int_{y_{j-\frac{1}{2}}}^{y_{j+\frac{1}{2}}} \int_{w_{k-\frac{1}{2}}}^{w_{k+\frac{1}{2}}} \int_{\mu_{m-\frac{1}{2}}}^{\mu_{m+\frac{1}{2}}} g_5 \dot{\Phi} v_h^\mp(x, y, w, \mu, \varphi_{n\pm\frac{1}{2}}) dx\, dy\, dw\, d\mu,$

where $\check{\Phi}, \bar{\Phi}, \widehat{g_3 \Phi}, \widetilde{g_4 \Phi}, \dot{\Phi}$ are the upwind numerical fluxes. The Poisson equation is solved by the local DG methods [11] with suitable boundary conditions. We refer further details of the schemes to [8].

## NUMERICAL RESULTS

Here we show the simulation results for a double gate MOSFET device as in Figure 1. The top and bottom shadowed region denotes the oxide-silicon region, whereas the rest is the silicon region. The relative dielectric constant in the oxide-silicon region is $\varepsilon_r = 3.9$, in the silicon region is $\varepsilon_r = 11.7$. We will only need to compute for $y > 0$ because of the symmetry of the problem. The electric potential is $\Psi = 0V$ at source, $\Psi = 2V$ at drain and $\Psi = 0.5V$ at gate. The boundary conditions for source and drain contacts as proposed in [4] have been implemented. For the interface of silicon and oxide-silicon region, we use simple specular reflection. The doping profile has been specified as follows: $N_D(x,y) = 10^{17} cm^{-3}$ if $x < 50nm$ or $x > 100nm$, $N_D(x,y) = 5 \times 10^{14} cm^{-3}$ in the channel $50nm \le x \le 100nm$. We use a very coarse mesh, $24 \times 12$ grid in space, 100 points in $w$, 8 points in $\mu$ and 6 points in $\varphi$ in our calculation. In Figure 2, we show macroscopic quantities for this device during the transient.

We consider also a 1D device of length $250nm$. The electric potential is $\Psi = 0V$ at source and $\Psi = 1V$ at drain and the doping profile is $N_D(x) = 5 \times 10^{18} cm^{-3}$ if $x < 100nm$ or $x > 150nm$ and $N_D(x) = 10^{15} cm^{-3}$ in the channel. The results are compared with DSMC data. Figure 3 show hydrodynamical variables and Fig. 4 the pdf near the second junction. All numerical results are obtained with piecewise linear polynomials and second order TVD Runge-Kutta time stepping.

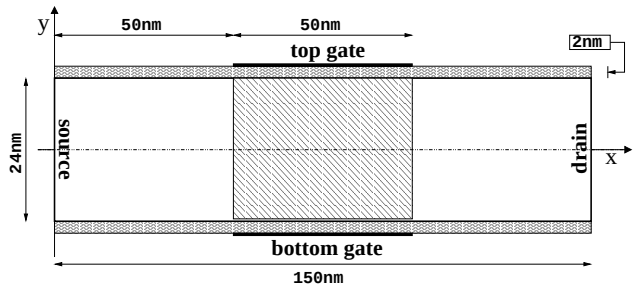


**FIGURE 1.** Schematic representation of a 2D double gate MOSFET device.

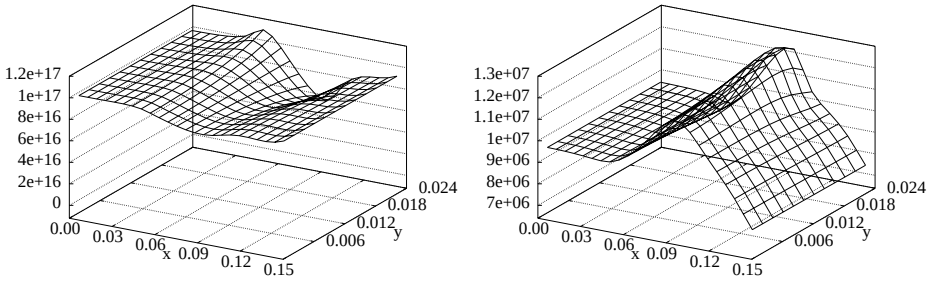


**FIGURE 2.** 2D double gate MOSFET at t = 0.8ps. Density in $cm^{-3}$ and the modulus of the velocity in $cm/s$.

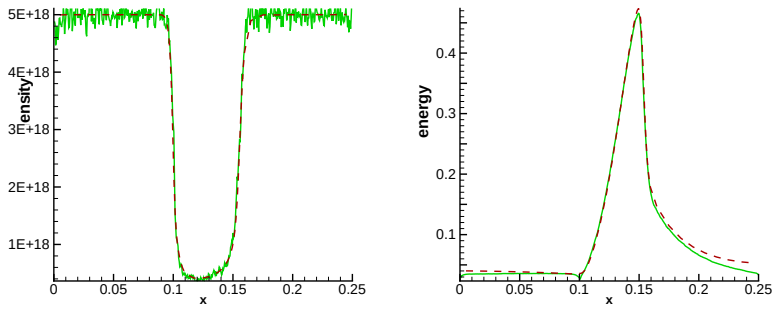


**FIGURE 3.** Comparison of macroscopic quantities using DG (dashed line) and DSMC (solid line) at $t = 3.0$ps. Left: density in $cm^{-3}$; right: energy in $eV$.

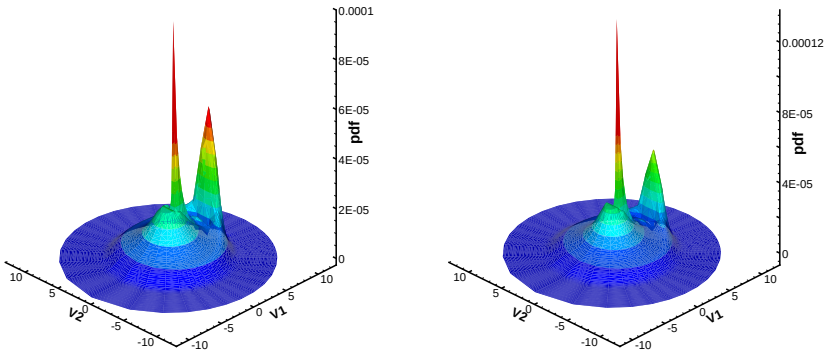


**FIGURE 4.** Non equilibrium PDF states near the drain junction at $t = 3.0$ps. They exhibit the large deviation from classical statistical states even at places corresponding to highly doped region. This is a signature of hot electron transport. Left: $x = 0.149\mu m$. Right: $x = 0.15\mu m$.

## EXTENSIONS AND FURTHER CONSIDERATIONS

It is well known that the transport Boltzmann equation associated with the BP system conserves mass, and the initial value problem propagates positivity. In particular, it is essential that the numerical schemes preserve these physical properties of the system. We can see easily that the DG scheme conserves mass in semi-discrete sense by plugging in the test function to be $v_h = 1$. From a simple argument [10, 12] follows that if the electric field stays under control, then a first order DG scheme will be monotone, hence preserves positivity. In addition, a high order accurate, positivity-preserving DG scheme for the Vlasov-Boltzmann transport equation was developed in [12], using a maximum-principle satisfying limiter technique for conservation laws [13]. In future work, we will explore this scheme in the setting of BP systems in the context of semiconductor device simulations.

Another important factor of the BP system is the band structure. The aforementioned system uses analytical band models, which means the energy band function $\varepsilon(\mathbf{k})$ has been given explicitly. The analytical band makes use of the explicit dependence of the carrier energy on the quasimomentum, which significantly simplifies all expressions as well as implementation of these techniques. However, the physical details of the band structure, when hot carriers in high-field phenomena are considered, are partly or totally ignored.

Full band models [14], on the other hand, can guarantee accurate physical pictures of the energy-band function. They are widely used in DSMC simulators, but only recently the Boltzmann transport equation was considered [15, 16], where approximate solutions were found by means of spherical harmonics expansion of the distribution function $f$. Since only a few terms of the expansion are usually employed, high order accuracy is not always achieved [17]. Recently in [9], the authors developed a DG code, which is the first deterministic code that can compute the full band model directly. The energy band is treated as a numerical input that can be obtained either by experimental data or the empirical pseudopotential method. The Dirac delta functions in the scattering kernels can be computed directly, based on the weak formulations of the PDE. The results in [9] for 1D devices have demonstrated the importance of using full band model when accurate description of macroscopic quantities under large applied bias is desired.

## ACKNOWLEDGMENTS

The first and second authors are partially supported by NSF DMS 1016001, 0757450 and 0807712. The third author thanks the support from the J. Tinsley Oden Faculty Research Fellowship and PRA 2009 Unict. The fourth author is supported by NSF DMS 0809086 and DOE DE-FG02-08ER25863. Support from the Institute for Computational Engineering and Sciences at the University of Texas at Austin is also gratefully acknowledged.

## REFERENCES

1. E. Fatemi, and F. Odeh, *J. Comput. Phys.* **108**, 209–217 (1993).
2. A. Majorana, and R. Pidatella, *J. Comput. Phys.* **174**, 649–668 (2001).
3. J. A. Carrillo, I. M. Gamba, A. Majorana, and C.-W. Shu, *J. Comput. Phys.* **184**, 498–525 (2003).
4. J. A. Carrillo, I. M. Gamba, A. Majorana, and C.-W. Shu, *J. Comput. Phys.* **214**, 55–80 (2006).
5. B. Cockburn, and C.-W. Shu, *J. Sci. Comput.* **16**, 173–261 (2001).
6. Y. Cheng, I. M. Gamba, A. Majorana, and C.-W. Shu, *SISPAD 07, June 14-17* pp. 257–260 (2007).
7. Y. Cheng, I. M. Gamba, A. Majorana, and C.-W. Shu, *J. Comput. Electron.* **7**, 119–123 (2008).
8. Y. Cheng, I. M. Gamba, A. Majorana, and C.-W. Shu, *Comput. Methods Appl. Mech. Eng.* **198**, 3130–3150 (2009).
9. Y. Cheng, I. M. Gamba, A. Majorana, and C.-W. Shu, *the Proceeding of IWCE13* pp. 211–214 (2009).
10. Y. Cheng, I. M. Gamba, A. Majorana, and C.-W. Shu, *Boletin de la Sociedad Espanola de Matematica Aplicada* (2010), preprint submitted.
11. B. Cockburn, and C.-W. Shu, *SIAM J. Numer. Anal.* **35**, 2440–2463 (1998).
12. Y. Cheng, I. M. Gamba., and J. Proft (2010), preprint submitted to Mathematics of Computation.
13. X. Zhang and C.-W. Shu, *J. Comput. Phys.* **229**, 3091-3120 (2010).
14. M. L. Cohen, and J. Chelikowsky, *Electronic Structure and Optical Properties of Semiconductors*, Springer-Verlag, 1989.
15. M. C. Vecchi, D. Ventura, A. Gnudi, and G.Baccarani, *Proceedings of NUPAD V Conference* **8**, 55–58 (1994).
16. S. Smirnov, and C. Jungemann, *J. Appl. Phys.* **99**, 063707 (1988).
17. A. Majorana, *Progress in Industrial Mathematics at ECMI 2000 - Mathematics in Industry* **1**, 169–173 (2002).